Electronic Supplementary Information

π⋯π interaction directed 2D FeNi-LDHs nanosheets from 2D Hofmann-MOFs for oxygen evolution reaction

Jia-Min Huo,[a] Ying Wang,[a]*, Jie Meng,[a] Xin-Yi Zhao,[a] Quan-Guo Zhai,[a] Yu-Cheng Jiang,[a] Man-Cheng Hu,[a] Shu-Ni Li,[a]* and Yu Chen[b]

[a] Key Laboratory of Macromolecular Science of Shaanxi Province, School of Chemistry & Chemical Engineering, Shaanxi Normal University, Xi'an, Shaanxi, 710062, China
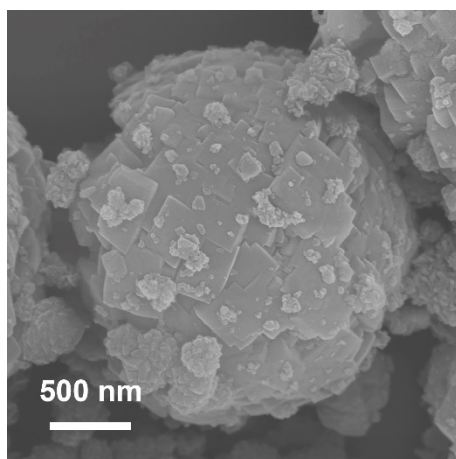
[b] School of Materials Science and Engineering, Shaanxi Normal University, Xi'an 710062, PR China
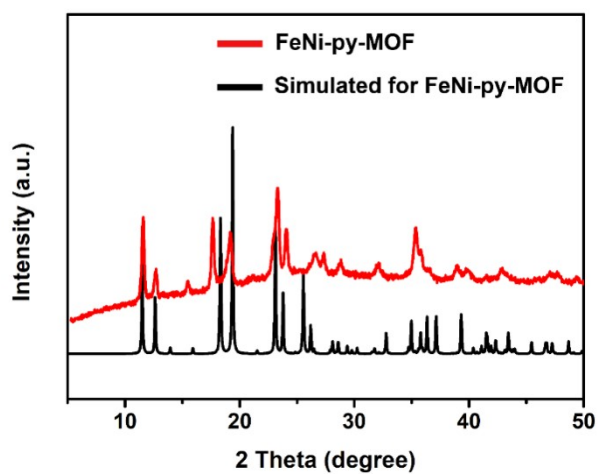
*Corresponding author

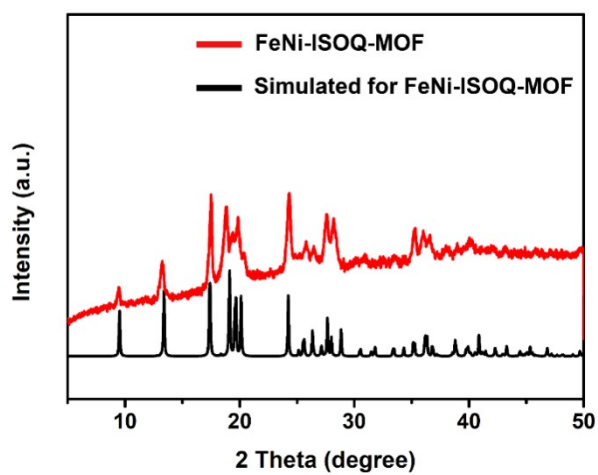Email: lishuni@snnu.edu.cn; wangyingyoyo@snnu.edu.cn
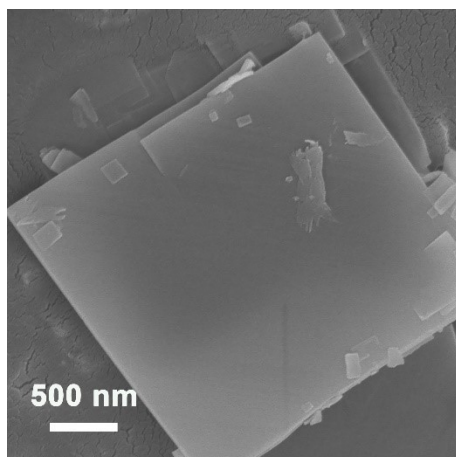
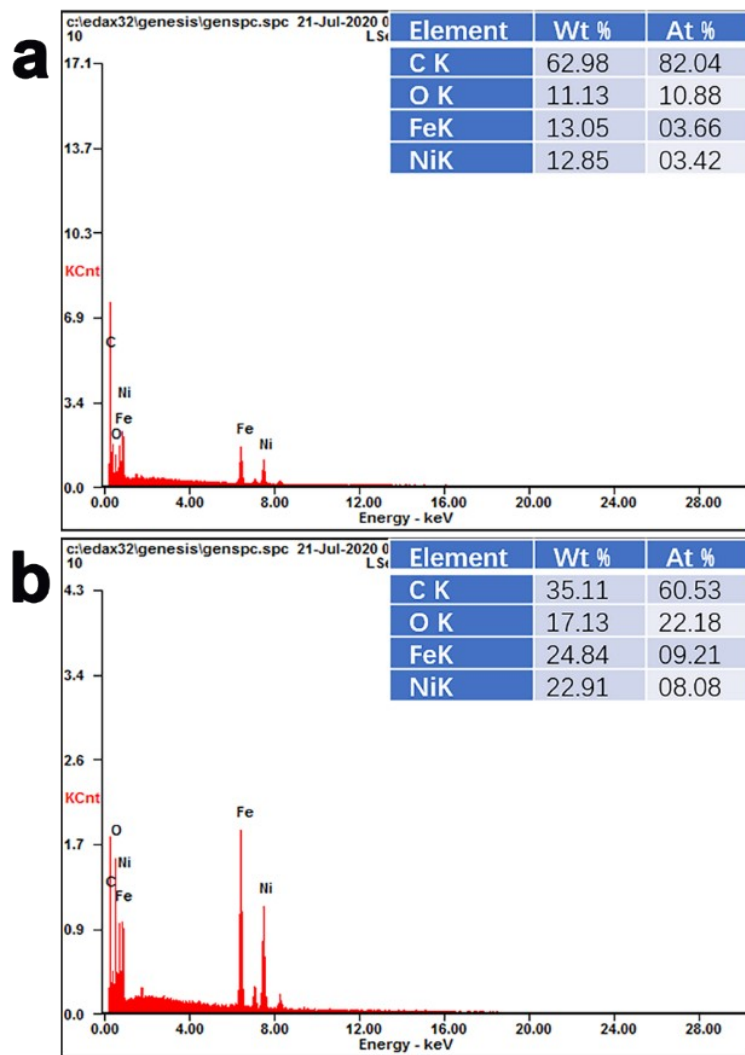**Figure S1.** SEM image of FeNi-py-MOF precursor.

Figure S2. SEM image of FeNi-ISOQ-MOF precursor.

Figure S3. XRD pattern of FeNi-py-MOF precursor.

Figure S4. XRD pattern of FeNi-ISOQ-MOF precursor.

a

Element	Wt %	At %
C K	62.98	82.04
O K	11.13	10.88
FeK	13.05	03.66
NiK	12.85	03.42

b

Element	Wt %	At %
C K	35.11	60.53
O K	17.13	22.18
FeK	24.84	09.21
NiK	22.91	08.08

Figure S5. EDX patterns of (a) FeNi-py-MOF and (b) FeNi-ISOQ-MOF precursors.

a

c:\edax32\genesis\genspc.spc 28-Aug-2020
LSec

Element	Wt %	At %
C K	60.02	74.81
N K	14.64	15.65
O K	04.33	04.05
FeK	10.05	02.69
NiK	10.95	02.79

b

c:\edax32\genesis\genspc.spc 28-Aug-2020
LSec

Element	Wt %	At %
C K	58.38	71.96
N K	17.76	18.78
O K	04.65	04.30
FeK	08.81	02.34
NiK	10.40	02.62
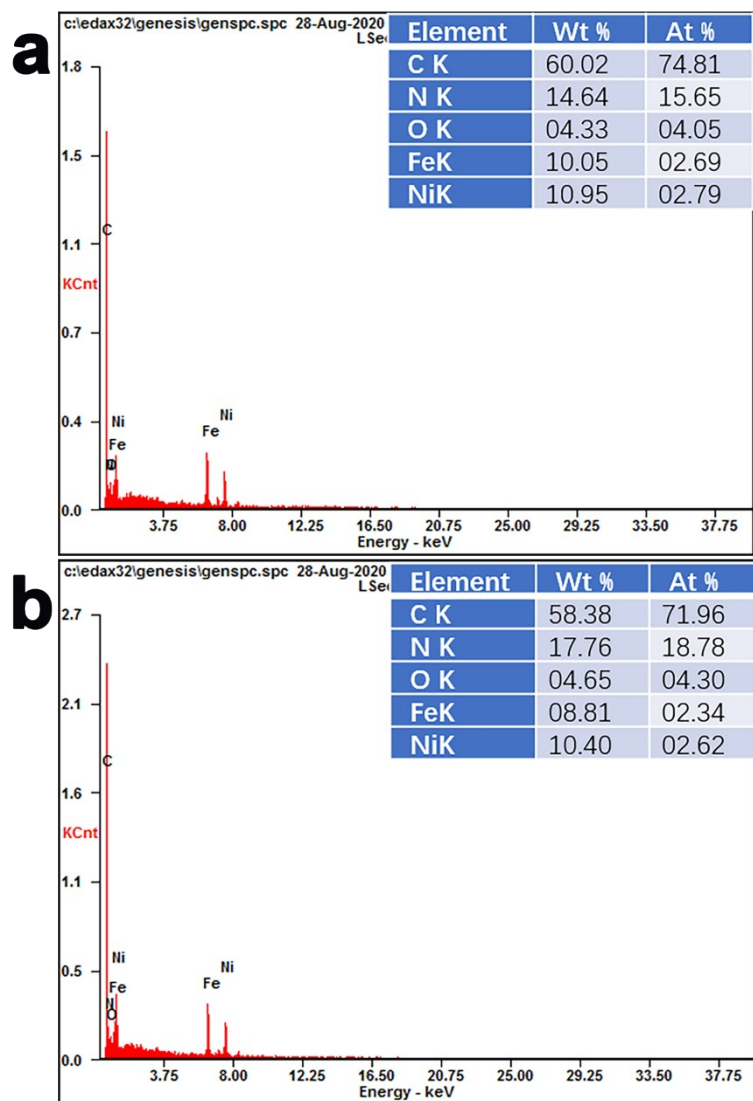
Figure S6. EDX patterns of (a) FeNi-py-LDH and (b) FeNi-ISOQ-LDH.
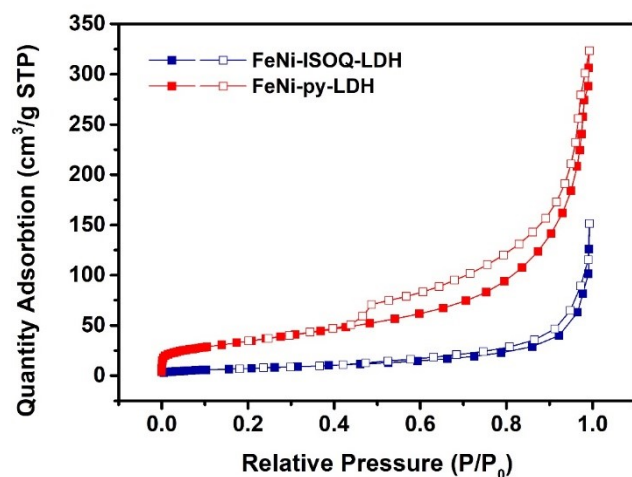
Figure S7. N_2 adsorption and desorption isotherms of FeNi-py-LDH and FeNi-ISOQ-LDH at 77 K.
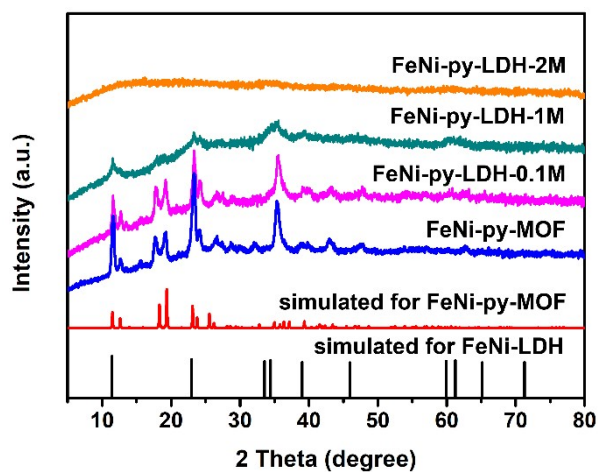
Figure S8. XRD patterns of FeNi-py-LDH-0.1M, FeNi-py-LDH-1M and FeNi-py-LDH-2M.

Figure S9. SEM image of FeNi-py-LDH-0.1M.

Figure S10. SEM image of FeNi-py-LDH-2M.
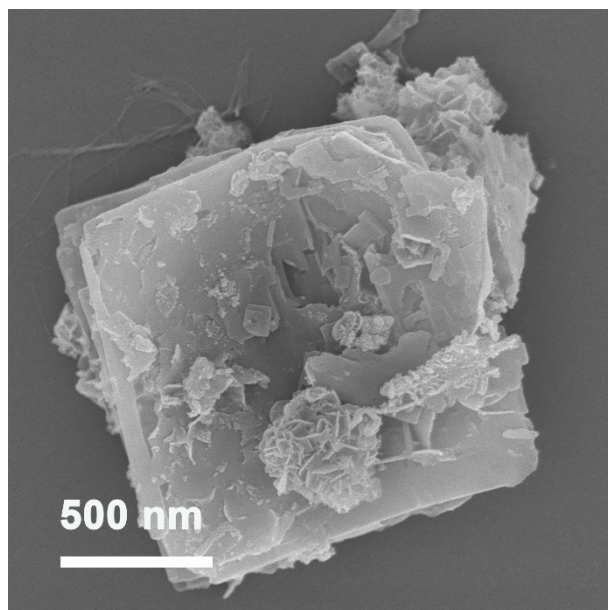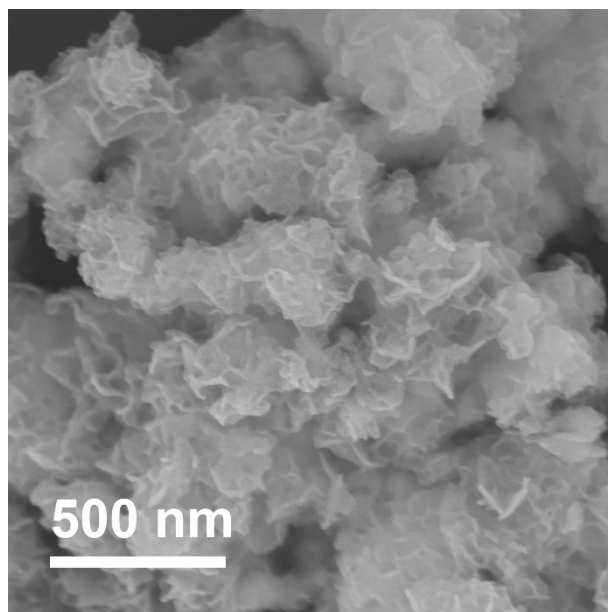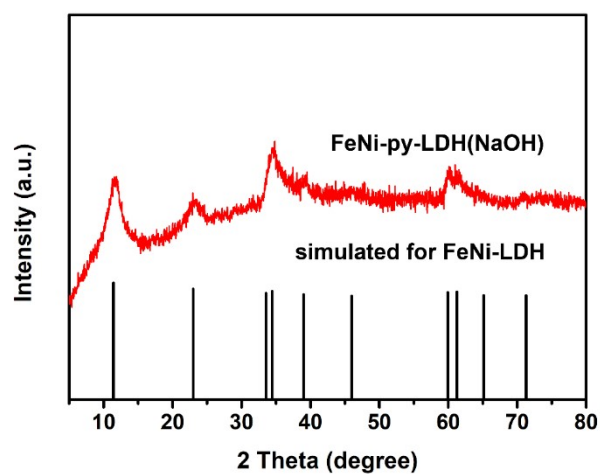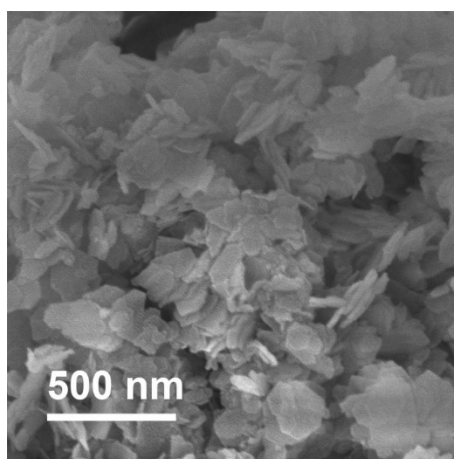
Figure S11. XRD patterns of FeNi-py-LDH(NaOH) and the simulated FeNi-LDH.

Figure S12. SEM image of FeNi-py-LDH(NaOH).
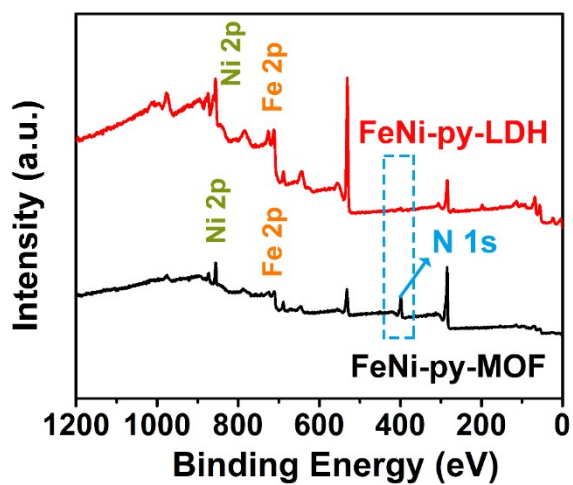
Figure S13. Survey XPS spectra of FeNi-py-MOF and FeNi-py-LDH.
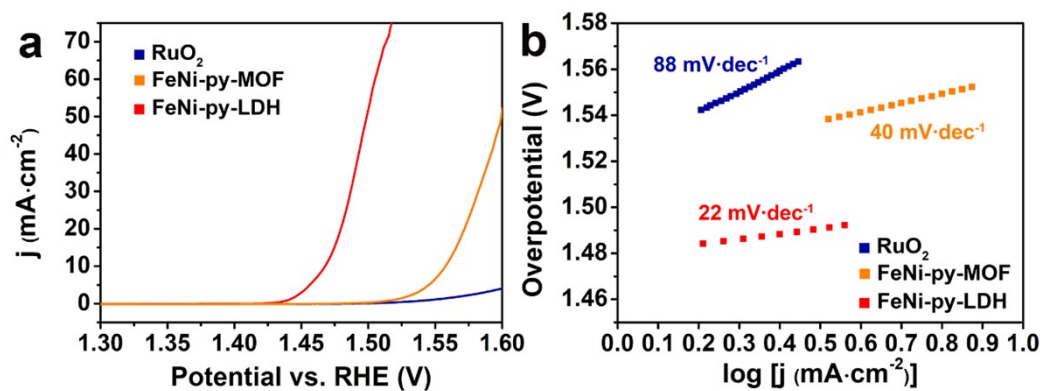
Figure S14. (a) The LSV curves of FeNi-py-LDH, FeNi-py-MOF and RuO$_2$. (b) The Tafel slopes of FeNi-py-LDH, FeNi-py-MOF and RuO$_2$.
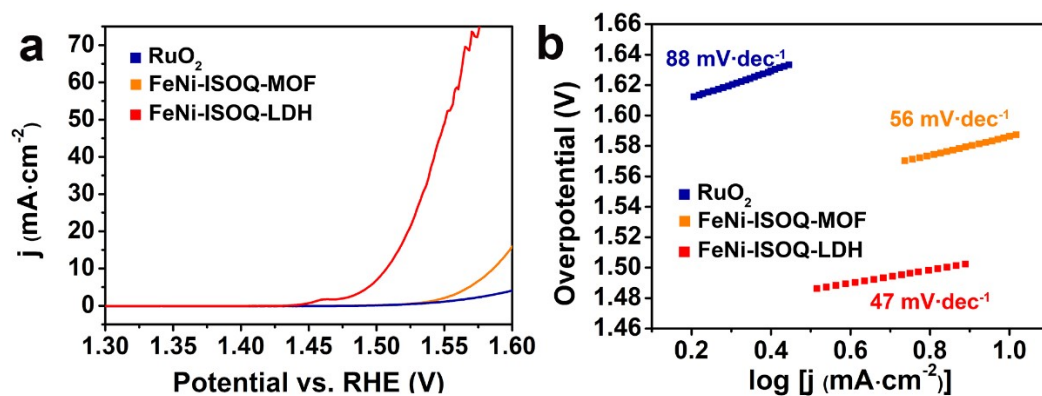
Figure S15. (a) The LSV curves of FeNi-ISOQ-LDH, FeNi-ISOQ-MOF and RuO$_2$. (b) The Tafel slopes of FeNi-ISOQ-LDH, FeNi-ISOQ-MOF and RuO$_2$.
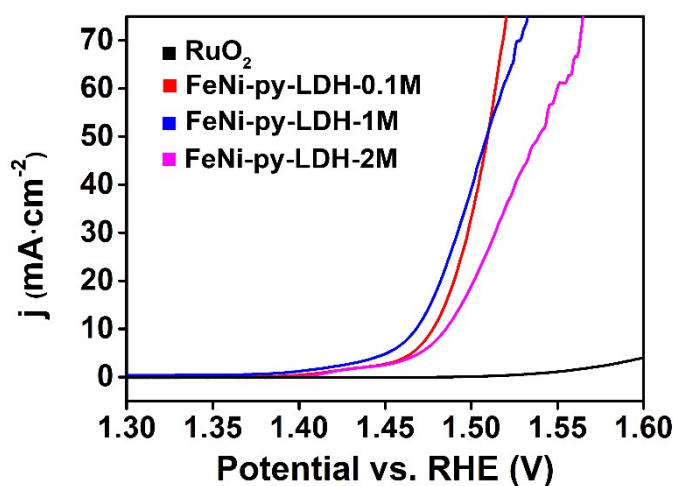
Figure S16. The LSV curves of FeNi-py-LDH-0.1M, FeNi-py-LDH-1M and FeNi-py-LDH-2M.
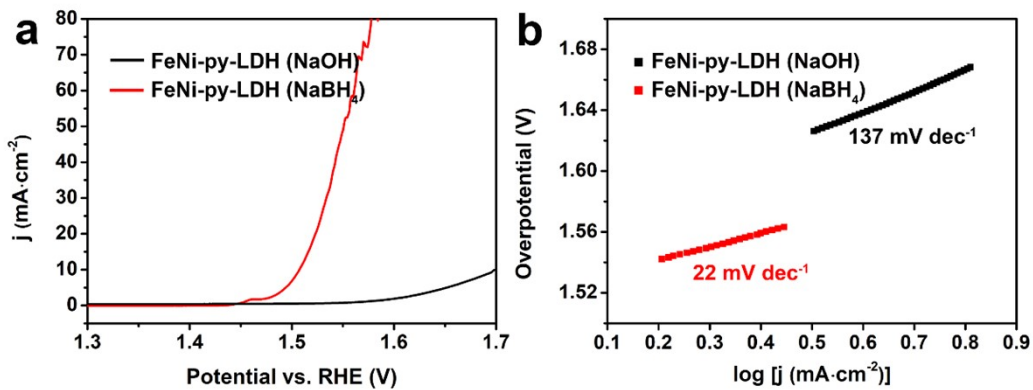
Figure S17. (a) The LSV curves of FeNi-py-LDH(NaOH) and FeNi-py-LDH(NaBH$_4$).
(b) The Tafel slopes of FeNi-py-LDH(NaOH) and FeNi-py-LDH(NaBH$_4$).
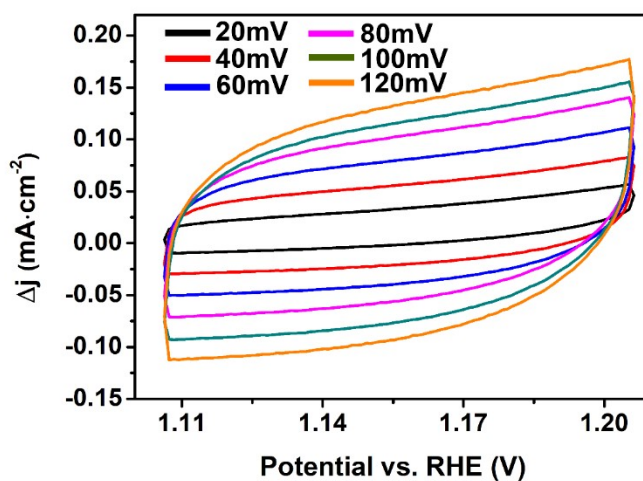
Figure S18. The CV curves of FeNi-py-LDH at different scan rate of 20, 40, 60, 80, 100 and 120 mV s^{-1}.
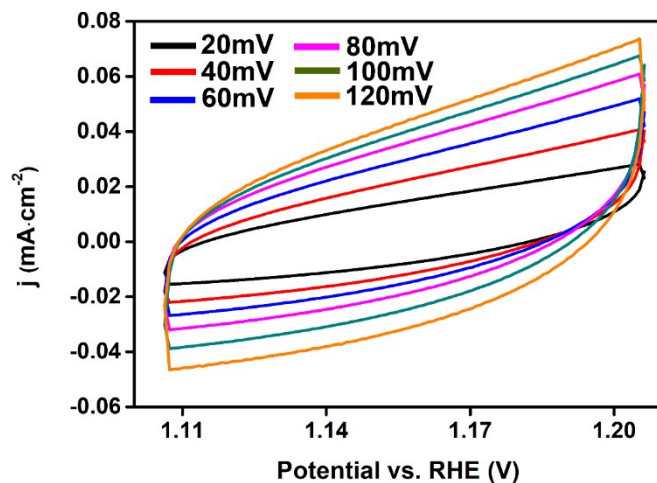
Figure S19. The CV curves of FeNi-ISOQ-LDH at different scan rate of 20, 40, 60, 80, 100 and 120 mV s⁻¹.
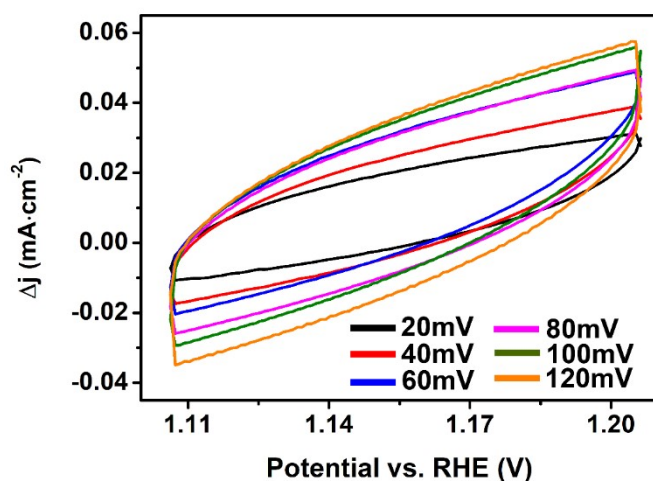
Figure S20. The CV curves of RuO$_2$ at different scan rate of 20, 40, 60, 80, 100 and 120 mV s⁻¹.

Figure S21. (a) XRD pattern and (b) SEM image of FeNi-py-LDH after 1000 cycles.
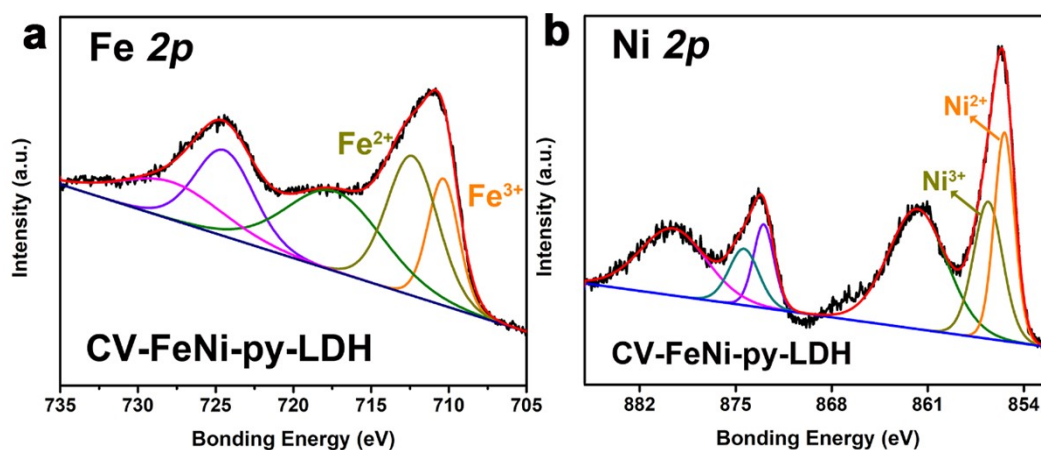
Figure S22. (a) Fe 2p (b) Ni 2p XPS spectra of FeNi-py-LDH after 1000 cycles.

Table S1. Comparison of electrocatalytic performance of OER catalysts in 1 M KOH.

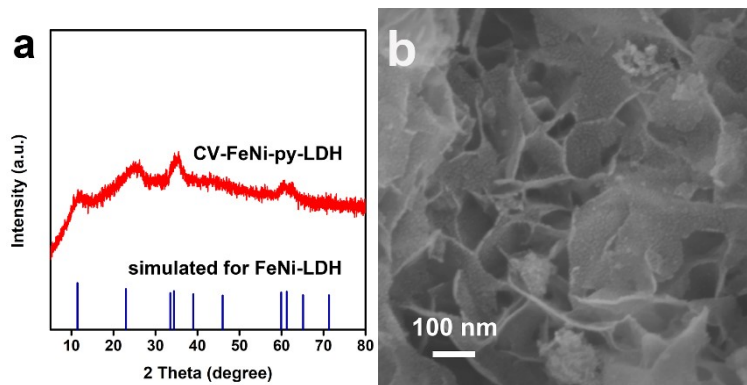| Catalysts	MOFs	Overpotential at 10 mA·cm^{-2} (mV)	Tafel slope (mV·dec^{-1})	C_{dl} (mF cm^{-2})	Ref.
FeNi-py-LDH	FeNi-py-MOF	238	22	1.9	This work
FeNi-ISOQ-LDH	FeNi-ISOQ-MOF	278	42	1.1	This work
RuO$_2$ nanoparticles	-	389	88	0.2	This work
Co$_9$S$_8$@NiFe LDH	-	220	52	31.8	[1]
Ni-Fe LDH-V$_O$	-	230	39.6	-	[2]
NiFeV-LDH	-	241	53.7	-	[3]
Ce-Ni-Fe LDH	MIL-88A	242	34	1.46	[4]
Ni-Fe DSNCs	MIL-88B	246(20 mA·cm^{-2})	71	1.46	[5]
NiFeCo-LDH/CF	ZIF-67	249	42	0.71	[6]
Fe-Ni@NC		257	54.6	5.58	[7]
Co$_8$Fe$_1$-LDH	-	262	42	0.59	[8]
Fe$_2$O$_3$@NiMOF-74	Ni-MOF-74	264	48	3.33	[9]
Co(OH)$_2$	-	267	62	-	[10]
Ni-Fe-OH/Ni$_3$S$_2$/NF		268	54	30.6	[11]
Fe-Ni LDH		280	49.4	-	[12]
γ-FeOOH/NF-6M	-	286	51	-	[13]
NiFe-LDH/NEGF		290	68	7.9	[14]
NaBH$_4$-FeNi-LDH		307	48		[15]
FeNiPc-CP	-	317	-	95	[16]
NCO-HNSs	-	340	51	-	[17]
FeOOH HNTAs	-	350	79	-	[18]

RuO$_2$ nanoparticles	-	370	-	-	[19]
RuO$_2$ nanoparticles		389	-	-	[20]
RuO$_2$ nanoparticles		390	-	-	[21]
RuO$_2$ nanoparticles		397	-	-	[22]
Beta-FeOOH	-	400	186	-	[23]
RuO$_2$ nanoparticles	-	400	-	-	[24]
NiOOH	-	453	189	3.4	[25]

REFERENCES

(1) Feng, X. T.; Jiao, Q. Z.; Dai, Z.; Dang, Y. L.; Suib, S. L.; Zhang, J. T.; Zhao, Y.; Li, H. S.; Feng, C. H.; Li, A. R. Revealing the effect of interfacial electron transfer in heterostructured Co$_9$S$_8$@NiFe LDH for enhanced electrocatalytic oxygen evolution. *J. Mater. Chem. A* **2021,** *9* (20), 12244-12254.

(2) Zhou, Y.; Zhang, W.; Hu, J.; Li, D.; Yin, X.; Gao, Q. Inherent Oxygen Vacancies Boost Surface Reconstruction of Ultrathin Ni-Fe Layered-Double-Hydroxides toward Efficient Electrocatalytic Oxygen Evolution. *ACS Sustain. Chem. Eng.* **2021,** *9* (21), 7390-7399.

(3) Zhou, L.; Zhang, C.; Zhang, Y.; Li, Z.; Shao, M. Host Modification of Layered Double Hydroxide Electrocatalyst to Boost the Thermodynamic and Kinetic Activity of Oxygen Evolution Reaction. *Adv. Funct. Mater.* **2021,** *31* (15), 2009743-2009753.

(4) Xu, H. J.; Shan, C. F.; Wu, X. X.; Sun, M. Z.; Huang, B. L.; Tang, Y.; Yan, C. H. Fabrication of layered double hydroxide microcapsules mediated by cerium doping in metal-organic frameworks for boosting water splitting. *Energy Environ. Sci.* **2020,** *13* (9), 2949-2956.

(5) Zhang, J.; Yu, L.; Chen, Y.; Lu, X. F.; Gao, S.; Lou, X. W. Designed Formation of Double-Shelled Ni–Fe Layered-Double-Hydroxide Nanocages for Efficient Oxygen Evolution Reaction. *Adv. Mater.* **2020,** *32* (16), 1906432-1906438.

(6) Lin, Y.; Wang, H.; Peng, C.; Bu, L.; Chiang, C.; Tian, K.; Zhao, Y.; Zhao, J.; Lin, Y.; Lee, J.; Gao, L. Co-Induced Electronic Optimization of Hierarchical NiFe LDH for Oxygen Evolution. *Small* **2020,** *16* (38), 2002426-2002435.

(7) Wang, Q. Q.; Song, Y. Y.; Sun, D. S.; Zhang, L. X. MOF-Derived Fe-Doped Ni@NC Hierarchical Hollow Microspheres as an Efficient Electrocatalyst for Alkaline Oxygen Evolution Reaction. *Acs Omega* **2021,** *6* (16), 11077-11082.

(8) Zhao, J.; Wang, X. R.; Chen, F. W.; He, C.; Wang, X. J.; Li, Y. P.; Liu, R. H.; Chen, X. M.; Hao, Y. J.; Yang, M.; Li, F. T. A one-step synthesis of hierarchical porous CoFe-layered double hydroxide nanosheets with optimized composition for enhanced oxygen evolution electrocatalysis. *Inorg. Chem. Front.* **2020,** *7* (3), 737-745.

(9) Gao, Z.; Yu, Z. W.; Liu, F. Q.; Yu, Y.; Su, X. M.; Wang, L.; Xu, Z. Z.; Yang, Y. L.; Wu, G. R.; Feng, X. F.; Luo, F. Ultralow-Content Iron-Decorated Ni-MOF-74 Fabricated by a Metal–Organic

Framework Surface Reaction for Efficient Electrocatalytic Water Oxidation. *Inorganic Chemistry* **2019,** *58* (17), 11500-11507.

(10) Liu, W.; Yin, R.; Shi, W.; Xu, X.; Shen, X.; Yin, Q.; Xu, L.; Cao, X. Gram-Scale Preparation of 2D Transition Metal Hydroxide/Oxide Assembled Structures for Oxygen Evolution and Zn-Air Battery. *ACS Appl. Energy Mater.* **2019,** *2* (1), 579-586.

(11) He, W. J.; Ren, G.; Li, Y.; Jia, D. B.; Li, S. Y.; Cheng, J. N.; Liu, C. C.; Hao, Q. Y.; Zhang, J.; Liu, H. Amorphous nickel-iron hydroxide films on nickel sulfide nanoparticles for the oxygen evolution reaction. *Catal. Sci. Technol.* **2020,** *10* (6), 1708-1713.

(12) Yu, L.; Yang, J. F.; Guan, B. Y.; Lu, Y.; Lou, X. W. Hierarchical Hollow Nanoprisms Based on Ultrathin Ni-Fe Layered Double Hydroxide Nanosheets with Enhanced Electrocatalytic Activity towards Oxygen Evolution. *Angew. Chem. Int. Ed.* **2018,** *57* (1), 172-176.

(13) Wang, K.; Du, H.; He, S.; Liu, L.; Yang, K.; Sun, J.; Liu, Y.; Du, Z.; Xie, L.; Ai, W.; Huang, W. Kinetically Controlled, Scalable Synthesis of γ-FeOOH Nanosheet Arrays on Nickel Foam toward Efficient Oxygen Evolution: The Key Role of In-Situ-Generated γ-NiOOH. *Adv. Mater.* **2021,** *33* (11), 2005587-2005596.

(14) Manna, N.; Ayasha, N.; Singh, S. K.; Kurungot, S. A NiFe layered double hydroxide-decorated N-doped entangled-graphene framework: a robust water oxidation electrocatalyst. *Nanoscale Adv.* **2020,** *2* (4), 1709-1717.

(15) Wang, Y. Q.; Tao, S.; Lin, H.; Han, S. B.; Zhong, W. H.; Xie, Y. S.; Hu, J.; Yang, S. H. $NaBH_4$ induces a high ratio of Ni^{3+}/Ni^{2+} boosting OER activity of the NiFe LDH electrocatalyst. *RSC Adv.* **2020,** *10* (55), 33475-33482.

(16) Qi, D.; Chen, X.; Liu, W.; Liu, C.; Liu, W.; Wang, K.; Jiang, J. A Ni/Fe-based heterometallic phthalocyanine conjugated polymer for the oxygen evolution reaction. *Inorg. Chem. Front.* **2020,** *7* (3), 642-646.

(17) Wang, H.; Hsu, Y.; Chen, R.; Chan, T.; Chen, H.; Liu, B. Ni^{3+}-Induced Formation of Active NiOOH on the Spinel Ni–Co Oxide Surface for Efficient Oxygen Evolution Reaction. *Adv. Energy Mater.* **2015,** *5* (10), 1500091-1500098.

(18) Feng, J.; Xu, H.; Dong, Y.; Ye, S.; Tong, Y.; Li, G. FeOOH/Co/FeOOH Hybrid Nanotube Arrays as High-Performance Electrocatalysts for the Oxygen Evolution Reaction. *Angew. Chem. Int. Ed.* **2016,** *55* (11), 3694-3698.

(19) Xu, X.; Zhong, Z.; Yan, X.; Kang, L.; Yao, J. Cobalt layered double hydroxide nanosheets synthesized in water–methanol solution as oxygen evolution electrocatalysts. *J. Mater. Chem. A* **2018,** *6* (14), 5999-6006.

(20) Han, X.; Yu, C.; Zhou, S.; Zhao, C.; Huang, H.; Yang, J.; Liu, Z.; Zhao, J.; Qiu, J. Ultrasensitive Iron-Triggered Nanosized Fe–CoOOH Integrated with Graphene for Highly Efficient Oxygen Evolution. *Adv. Energy Mater.* **2017,** *7* (14), 1602148-1602156.

(21) Zhang, J.; Zhang, M.; Qiu, L.; Zeng, Y.; Chen, J.; Zhu, C.; Yu, Y.; Zhu, Z. Three-dimensional interconnected core–shell networks with Ni(Fe)OOH and M–N–C active species together as high-efficiency oxygen catalysts for rechargeable Zn–air batteries. *J. Mater. Chem. A* **2019,** *7* (32), 19045-19059.

(22) Zou, H.; He, B.; Kuang, P.; Yu, J.; Fan, K. Metal–Organic Framework-Derived Nickel–Cobalt Sulfide on Ultrathin Mxene Nanosheets for Electrocatalytic Oxygen Evolution. *ACS Appl. Mater. Interfaces* **2018,** *10* (26), 22311-22319.

(23) Liang, Y.; Yu, Y.; Huang, Y.; Shi, Y.; Zhang, B. Adjusting the electronic structure by Ni

incorporation: a generalized in situ electrochemical strategy to enhance water oxidation activity of oxyhydroxides. *J. Mater. Chem. A* **2017,** *5* (26), 13336-13340.

(24) Li, P.; Wang, M.; Duan, X.; Zheng, L.; Cheng, X.; Zhang, Y.; Kuang, Y.; Li, Y.; Ma, Q.; Feng, Z.; Liu, W.; Sun, X. Boosting oxygen evolution of single-atomic ruthenium through electronic coupling with cobalt-iron layered double hydroxides. *Nat. Commun.* **2019,** *10* (1), 1711-1721.

(25) Huang, L.; He, Z.; Guo, J.; Pei, S.; Shao, H.; Wang, J. Photodeposition fabrication of hierarchical layered Co-doped Ni oxyhydroxide ($Ni_xCo_{1-x}OOH$) catalysts with enhanced electrocatalytic performance for oxygen evolution reaction. *Nano Res.* **2020,** *13* (1), 246-254.